



ELSEVIER

Contents lists available at ScienceDirect

Journal of Ginseng Research

journal homepage: <https://www.sciencedirect.com/journal/journal-of-ginseng-research/>

Research article

Saponins from *Panax japonicus* ameliorate age-related renal fibrosis by inhibition of inflammation mediated by NF- κ B and TGF- β 1/Smad signaling and suppression of oxidative stress via activation of Nrf2-ARE signaling

Yan Gao^{1,☆}, Ding Yuan^{1,☆}, Liyue Gai^{1,☆}, Xuelian Wu¹, Yue Shi¹, Yumin He¹, Chaoqi Liu¹, Changcheng Zhang¹, Gang Zhou², Chengfu Yuan^{1,3,*}

¹ College of Medical Science, China Three Gorges University, Yichang, China

² College of Traditional Chinese Medicine, China Three Gorges University, Yichang, China

³ Third-Grade Pharmacological Laboratory on Chinese Medicine Approved by State Administration of Traditional Chinese Medicine, China Three Gorges University, Yichang, China



ARTICLE INFO

Article history:

Received 14 April 2020

Received in Revised form

22 July 2020

Accepted 26 August 2020

Available online 9 September 2020

Keywords:

Total saponins of *panax japonicus*

Aging

Renal fibrosis

TGF- β 1/Smad

Nrf2-ARE signaling pathways

ABSTRACT

Background: The decreased renal function is known to be associated with biological aging, of which the main pathological features are chronic inflammation and renal interstitial fibrosis. In previous studies, we reported that total saponins from *Panax japonicus* (SPJs) can availably protect acute myocardial ischemia. We proposed that SPJs might have similar protective effects for aging-associated renal interstitial fibrosis. Thus, in the present study, we evaluated the overall effect of SPJs on renal fibrosis.

Methods: Sprague-Dawley (SD) aging rats were given SPJs by gavage beginning from 18 months old, at 10 mg/kg/d and 60 mg/kg/d, up to 24 months old. After the experiment, changes in morphology, function and fibrosis of their kidneys were detected. The levels of serum uric acid (UA), β 2-microglobulin (β 2-MG) and cystatin C (Cys C) were assayed with ELISA kits. The levels of extracellular matrix (ECM), matrix metalloproteinases (MMPs), tissue inhibitors of metalloproteinases (TIMPs), inflammatory factors and changes of oxidative stress parameters were examined.

Results: After SPJs treatment, SD rats showed significantly histopathological changes in kidneys accompanied by decreased renal fibrosis and increased renal function; As compared with those in 3-month group, the levels of serum UA, Cys C and β 2-MG in 24-month group were significantly increased ($p < 0.05$). Compared with those in the 24-month group, the levels of serum UA, Cys C and β 2-MG in the SPJ-H group were significantly decreased. While ECM was reduced and the levels of MMP-2 and MMP-9 were increased, the levels of TIMP-1, TIMP-2 and transforming growth factor- β 1 (TGF- β 1)/Smad signaling were decreased; the expression level of phosphorylated nuclear factor kappa-B (NF- κ B) was down-regulated with reduced inflammatory factors; meanwhile, the expression of nuclear factor erythroid 2-related factor 2-antioxidant response element (Nrf2-ARE) signaling was aggrandized.

Conclusion: These results suggest that SPJs treatment can improve age-associated renal fibrosis by inhibiting TGF- β 1/Smad, NF κ B signaling pathways and activating Nrf2-ARE signaling pathways and that SPJs can be a potentially valuable anti-renal fibrosis drug.

© 2020 The Korean Society of Ginseng. Publishing services by Elsevier B.V. This is an open access article under the CC BY-NC-ND license (<http://creativecommons.org/licenses/by-nc-nd/4.0/>).

Abbreviations: SPJs, saponins from *panax japonicus*; NF- κ B, nuclear factor kappa-B; TGF- β 1, tumor growth factor- β 1; SD, Sprague-Dawley; ECM, extracellular matrix; MMPs, matrix metalloproteinases; TIMPs, tissue inhibitors of metalloproteinases; IL-6, interleukin-6; TNF- α , tumor necrosis factor- α ; MCP-1, monocyte chemoattractant protein-1; COX2, cyclooxygenase-2; I κ B, inhibitor of NF- κ B; LPO, lipid peroxides; Nrf2, nuclear factor erythroid 2-related factor 2; ARE, antioxidant response element; SPJ-L, low-dose of SPJ; SPJ-H, high-dose of SPJ; PJ, *Panax japonicus*; UA, uric acid; β 2-MG, β 2-microglobulin; Cys C, cystatin C; α -SMA, α -smooth muscle aorta; HO-1, human heme oxygenase 1; NQO1, recombinant NADH dehydrogenase quinone 1.

* Corresponding author. Department of Biochemistry, College of Medical Science, China Three Gorges University, Yichang, 443002, China.

E-mail address: yuancf46@ctgu.edu.cn (C. Yuan).

☆ These authors contributed equally to this work.

<https://doi.org/10.1016/j.jgr.2020.08.005>

p1226-8453 e2093-4947/\$ – see front matter © 2020 The Korean Society of Ginseng. Publishing services by Elsevier B.V. This is an open access article under the CC BY-NC-ND license (<http://creativecommons.org/licenses/by-nc-nd/4.0/>).

1. Introduction

Clinically, in patients with chronic kidney disease, their renal function is decreased with age and is frequently accompanied by structural changes in their kidneys [1]. Renal fibrosis is a primary impairment in age-associated, progressive renal disease [2], which imposes a heavy economic burden. Treatment of end-stage kidney disease usually costs about 2–3% of the annual health-care budget in developed countries. Worldwide, the total cost for treating the milder forms of chronic renal disease is higher than that for treating end-stage kidney disease. For instance, more than 64 billion and 34 billion U. S. dollars were spent on chronic and end-stage kidney disease, respectively, from medicare expenditures in USA in 2015. A large proportion of the expenditure, morbidity and mortality that were previously attributed to such chronic diseases as hypertension and diabetes are actually attributable to kidney disease and its complications [3]. The cellular mechanisms underlying age-associated renal fibrosis are very intricate, encompassing senescence, oxidative stress and inflammation etc [4]. Therefore, to discover and develop effective treatment strategies is of practical significance for appropriate adjustment in age-associated renal fibrosis.

The characteristic of renal fibrosis is progressive accumulation of extracellular matrix (ECM) proteins. At the same time, matrix metalloproteinases (MMPs), the multifunctional enzymes, can lyse basement membrane and ECM components. The activities of various MMPs can be regulated by a variety of mechanisms, such as inhibition of tissue inhibitors of metalloproteinases (TIMPs) [5,6]. Increasing body of evidence has indicated that transforming growth factor- β (TGF- β) signaling plays an important role in renal fibrosis. TGF- β 1 is believed to be a key intermediary of renal fibrosis by activating the downstream Smad signaling pathway [7,8]. TGF- β 1 is involved in initiation of renal fibrosis. Furthermore, ECM, MMPs and TIMPs further also participate in this process, together, their imbalance and malfunctions lead to renal fibrosis.

Chronic inflammation is a major risk factor contributing to the gradual development of renal fibrosis. Nevertheless, aging-associated chronic inflammation is characterized by several characteristics, including immune system disorders and increased oxidative stress. Thereinto, maladjustment of immune system is the main factor causing increased inflammation during the aging process [9,10]. The currently available evidence strongly suggests that chronic up-regulation of nuclear factor Kappa B (NF- κ B) induced by maladjustment of immune system stimulates the expression of pro-inflammatory factors, such as tumor necrosis factor- α (TNF- α), interleukin-1 β (IL-1 β), monocyte chemoattractant protein-1 (MCP-1), IL-6, cyclooxygenase-2 (COX2) and inducible nitric oxide synthases (iNOS), during the aging process. In inactive state, NF κ B protein is present in cytoplasm where it binds to inhibitor of NF- κ B (I κ B) protein; under stress, I κ B protein is degraded, then NF- κ B protein is released and transported into the nucleus within which it binds to the consensus κ B DNA motif of promoters and enhancers of target genes, initiating the inflammatory responses [11–13]. Furthermore, oxidative stress is also one of the mechanisms participated in the occurrence and development of age-associated renal fibrosis. Excessive reactive oxygen species (ROS) play a crucial part in a high level of oxidative stress. ROS, including hydrogen peroxide (H₂O₂), hydroxyl radicals, and superoxide anions, are produced in normal cell oxidative metabolism as well as malondialdehyde (MDA) and lipid peroxides (LPO), which are the products of membrane lipid peroxidation [14]. The activities of a number of antioxidant enzymes, including catalase (CAT), superoxide dismutase (SOD), glutathione-peroxidase (GSH-PX), and the levels of non-enzymatic antioxidants, such as glutathione (GSH), are associated with the regulation of production/degradation of

ROS [15]. Furthermore, nuclear factor erythroid 2-related factor 2 (Nrf2) can be directly bound to antioxidant response element (ARE) and is involved in conditioning of oxidative stress in cells through the Nrf2-ARE pathway [16].

Saponins is a class of phytochemicals present in various plant species, including *Panax japonicus* (*P. japonicus*). And the saponins and non-saponins in ginseng have important medicinal value [17]. The main components of SPJs include Ginsenoside Re, *panax japonicus* V, *panax japonicus* IV, *panax japonicus* IVa and *panax japonicus* 2. It has been reported that SPJs was capable of inhibiting cardiomyocyte apoptosis by AMP-activated protein kinase/Sirtuin 1/NF- κ B (AMPK/Sirt1/ NF- κ B) signaling pathway in aging rats [18] and attenuating age-related neuroinflammation through regulating the mitogen-activated protein kinase (MAPK)/ NF- κ B signaling pathways [19]. We found previously that SPJs could effectively inhibit inflammatory responses in myocardial tissue and the oxidative stress in brain tissue [20,21]. Thus, we hypothesized that SPJs might also have the similar effects on inhibiting inflammatory responses in kidneys. In present study, we monitored changes in morphology, function, oxidative stress, inflammation and the improvement of renal fibrosis of kidney tissues of the naturally aging rats after being treated with SPJs. Meanwhile, we also detected the underlying mechanisms by examining changes in the expression levels of the key genes involved in TGF- β /Smad, NF- κ B and Nrf2-ARE signaling pathways.

2. Materials and methods

2.1. Rats and administration with SPJs

In this research, a total of 48 naturally aging male Sprague Dawley (SD) rats were obtained from Laboratory Animal Centre of China Three Gorges University (Hubei, China). They were randomly divided into four groups: 3-month group (n = 12), 24-month group (n = 12), 24-month low-dose of SPJ group (SPJ-L) (n = 12) and 24-month high-dose of SPJ group (SPJ-H) (n = 12). The experimental rats were separately maintained in cages with greenhouses (22 \pm 2) $^{\circ}$ C, humidity (60 \pm 5)%, and a 12h light-12h dark cycle. All animal experiments were complied with the Experimental Animal Operating Standards of China Three Gorges University and were approved by the Ethics Committee of this university.

The roots of *P. japonicus* were purchased from Enshi Chunmuying Medicinal Materials Planting Base (Enshi, Hubei, China), and total saponins were extracted from the roots of *P. japonicus* with the extraction method of SPJs based on our previous research [22].

SPJs were dissolved in 1% sodium carboxymethyl cellulose just before use. According to the preliminary experiment, rats in SPJ-L group (10mg/kg/d) and SPJ-H group (60mg/kg/d) were administered with SPJs at the indicated doses by gavage beginning from the 18th month to the 24th month. In addition, rats in 3-month group (3-M) (orally, continuously for 3 months) and in 24-month (24-M) group (orally, continuously for 6 months) were given with 1% sodium carboxymethyl cellulose as the vehicle.

2.2. Histopathologic evaluation

In each group, 6 rats were anesthetized by intraperitoneally injecting 4% chloral hydrate (300 mg/kg body weight) and then perfused with 4% paraformaldehyde in 0.1M phosphate buffered saline (PBS) (pH7.4). After fixation with 4% paraformaldehyde in 0.1M PBS, the isolated renal tissues were conventionally embedded in paraffin. Paraffin sections of renal tissue (5 μ m) were dewaxed with xylene and dehydrated with gradient ethanol, then stained with hematoxylin and eosin (H&E). Changes in renal pathological

parameters were visualized with the light microscope (Olympus, BX61, Japan).

2.3. Masson's trichrome staining

The tissue slices of the same kidney samples as those used for histopathologic evaluation were stained with Masson's trichrome and the collagen deposition in kidneys was analyzed. The operation was carried out according to the instructions of Masson's trichrome staining kit (Beyotime Institute of Biotechnology, China). By using Image Pro Plus6.0 Image software, blue stained areas were quantitatively analyzed. Twenty different fields of vision were stochastically chosen from each section, and blue area of fiber was taken as the positive staining. The ratio of the positive area to the total field of vision was used as the renal fibrosis index.

2.4. Enzyme-linked immunosorbent assay (ELISA)

Blood samples of 6 rats in each group were collected. After centrifugation at 4°C at 1000 rpm for 5 min, serum samples were cryopreserved at -80°C. The levels of serum uric acid (UA), β_2 -microglobulin (β_2 -MG) and cystatin C (Cys C) were detected with corresponding ELISA kits by following the manufacturer's instructions. The ELISA kits (catalog numbers: SY-UA0111, SY- β_2 -MG0512, and SY-Cys-C0329) of rats were obtained from Shanghai Win-win Biotechnology co., LTD.

2.5. Detection of oxidative stress indexes

Renal tissues were homogenized with 10% (w/v) frozen 0.1M PBS (pH 7.4), and then centrifuged at 4°C and 3500 rpm for 15 min. Supernatants were gathered and subsequently used to detect the indexes of oxidative stress. The levels of MDA, GSH, LPO, GSH-PX, SOD and CAT were assayed by spectrophotometry through following instructions of the corresponding kits (catalog numbers: A003-1-2, A006-2-1, A106-1-3, A005-1-2, A001-3-2, and A007-1-1) purchased from Jiancheng Bioengineering Institute (Nanjing, Jiangsu, China).

2.6. Immunohistochemistry analysis

The renal tissue slices from the same kidney samples as those used for histopathologic evaluation were also taken for analyzing immunohistochemical staining. All the sections of kidney (4 μ m) were deparaffinized by xylene, hydrated by gradient ethanol, and incubated with 0.01M citrate buffer (pH 6.0) for antigen retrieval; then slices were soaked in 3% H₂O₂ to inactivate activity of endogenous peroxidase and blocked using 5% bovine serum albumin (BSA) at 25°C room temperature. Afterwards, sections were incubated at 4°C overnight by using primary antibodies specific for α -SMA (Santa Cruz Biotechnology, sc-53142, 1:500) and Vimentin (Santa Cruz Biotechnology, sc-6260, 1:500). After being washed with PBS buffer, slices were immediately incubated with corresponding secondary antibodies at room temperature for 1 h. After adding freshly prepared diaminobenzidine (DAB), they were counterstained with hematoxylin, differentiated with hydrochloric acid alcohol, dehydrated with gradient ethanol, and transparentized with xylene. Finally, the positive expression of tan was visualized under the microscope. Ten different fields were casually picked from each slice, and relative positive staining area was acquired by Image Pro Plus6.0.

Table 1
The primer sequences used for real-time PCR

Gene	Forward primer (5'-3')	Reverse primer (5'-3')
Nrf2	gacctaaagcacagccaacacat	ctcaatcggcttgaatgtttgtc
TGF- β 1	tgcgcttgacagattaaaa	agccctgtattccgtctctc
Smad2	aaccggaatgtgcaccataagaa	gcgagcttttgatgggtttacga
Smad3	ccccagagcaatattccaga	tgtgaagcgtggaatgtctc
Smad4	aaggcctagcaccaccttag	agccttaaaccttgacctgt
HO-1	tgtcccaggatttgcgag	actgggttctgctgtttcct
NQO1	ggggacatgaacgtcattctc	agtgtgactctcccagacag
TIMP1	gggcttcaccaagaccta	gaagaaagatgggagtgagg
TIMP2	ccaaagcggctcagtgaga	tggtgcccttgatgttc
MMP2	acttgatgccctcgtggac	tgtggcagcaccaggcagc
MMP9	cgctggcttagatcattcc	ttgtcggcgataaggaagg
Fibronectin	gactcgtttgactccaccac	tccttctcgtcagttcgt
Collagen I	actcagccttctgtcctca	ggagggcctggggacatta
Collagen III	aagggcaggaacaactgat	gtgaagcaggggtgagaagaaac
Collagen IV	cgggattactggaccacc	cccttgcctcctgtca
TNF- α	tgctctgtgaggcactgg	gggctctgaggagtagacataag
IL-1 β	ggaacagcaatggctggg	gacttggcagaggacaaaggc
IL-6	caacttccaatgctctctaatgg	tgccgagtagacctatagtgacc
GAPDH	aacttggcattgtggaagg	acacattggggtaggaaca

2.7. Analysis of mRNA levels of target genes with quantitative real time PCR (qRT-PCR)

Total RNA was extracted from renal tissues with TRIZOL reagent. Integrity was detected by running RNA samples on 1.2% agarose gel after DNase treated. The template cDNA was obtained by reverse transcription of 2 μ g total RNA. qRT-PCR reaction was carried out as follows: initial reaction was at 95°C for 10 min, then they were performed for 40 cycles of 95°C for 15 sec and 60°C for 1 min. Next, the relative expression levels of gene were calculated with 2^{- $\Delta\Delta$ Ct} method, by using GAPDH as an internal control. Specific primer sequences targeting Nrf2, TGF- β 1, Smad2, Smad3, Smad4, heme oxygenase-1 (HO-1), NAD(P)H dehydrogenase [quinone] 1 (NQO1), TIMP1, TIMP2, MMP2, MMP9, fibronectin, collagen I, collagen III, collagen IV, TNF- α , IL-1 β , and IL-6 with qRT-PCR analysis were shown in Table 1.

2.8. Analysis of protein expression levels of target proteins with Western blot

The collected renal tissues were homogenized with RIPA buffer. The homogenate was centrifugated at 4°C at 12000 rpm for 15 min and the supernatant was saved for subsequent analysis. The 50 μ g denatured proteins were isolated by running on sodium dodecyl sulfate poly-acrylamide gel electrophoresis (SDS-PAGE) and shifted to polyvinylidene difluoride (PVDF) film. Films containing proteins were soaked in 5% milk for 1h and then incubated at 4°C overnight with corresponding primary antibody. The sources and dilutions for antibodies for the target proteins, including anti-collagen-I, anti-collagen-III, anti-collagen-V, anti-MMP2, anti-MMP9, anti-TIMP1, anti-TIMP2, anti-TGF- β 1, anti-Smad 2/3, anti-Smad 4, anti-IL-6, anti-IL-1 β ; anti-TNF- α , Anti-phospho-NF- κ B, anti-NF- κ B; Anti-phospho-I κ B, anti-I κ B, anti-Nrf2, anti-HO1, anti-NQO1 and anti- β -actin, were listed in Table 2. After being washed with tris-buffered saline and Tween 20 (TBST) buffer for 3 times, target protein bands were detected by incubating with corresponding secondary antibody at 25°C room temperature for 1h; lastly, protein bands were displayed with electrochemiluminescence (ECL) reagent after washed. Images were acquired with Image-pro Plus 6.0. The expression level of each protein was individually normalized to that of β -actin and expressed as the fold changes in relative to the corresponding control.

Table 2
Antibodies, sources and dilutions used in this study

Name of antibody	Source/Cat. #	Dilutions	Method
Anti-Fibronectin	Abcam/ab45688	1:500	Immunostaining
Anti- α -SMA	Santa Cruz Biotechnology/sc-53142	1:500	Immunostaining
Anti-Vimentin	Santa Cruz Biotechnology/sc-6260	1:500	Immunostaining
Anti-collagen-I	Abcam/ab90395	1:1000	Western blot
Anti-collagen-III	Santa Cruz Biotechnology/sc-514601	1:500	Western blot
Anti-collagen-IV	Abcam/ab6586	1:1000	Western blot
Anti-MMP2	Abcam/ab37150	1:1000	Western blot
Anti-MMP9	Abcam/ab38898	1:2000	Western blot
Anti-TIMP1	Abcam/ab61224	1:1500	Western blot
Anti-TIMP2	Abcam/ab180630	1:1000	Western blot
Anti-TGF- β 1	Abcam/ab92486	1:1000	Western blot
Anti-Smad 2/3	Santa Cruz Biotechnology/sc-398844	1:1000	Western blot
Anti-Smad 4	Santa Cruz Biotechnology/sc-1909	1:1000	Western blot
Anti-IL-6	Santa Cruz Biotechnology/sc-57315	1:500	Western blot
Anti-IL-1 β	Abcam/ab9722	1:1000	Western blot
Anti-TNF- α	Santa Cruz Biotechnology/sc-52746	1:500	Western blot
Anti-Phospho-NF- κ B	cell signaling/No:6956	1:500	Western blot
Anti-NF- κ B	Santa Cruz Biotechnology/sc-365568	1:500	Western blot
Anti-phospho-I κ B	Abcam/ab12135	1:500	Western blot
Anti-I κ B	cell signaling/No:4812	1:1000	Western blot
Anti-Nrf2	Abcam/ab137550	1:1000	Western blot
Anti-HO1	Abcam/ab3243	1:1000	Western blot
Anti-NQO1	Abcam/ab28947	1:1000	Western blot
Anti- β -actin	Santa Cruz Biotechnology/sc-47778	1:1000	Western blot

2.9. Statistical analysis

All data were expressed as mean \pm standard deviation, and experimental datum was analyzed and processed by SPSS13.0, image-pro Plus6.0 software. The significant difference in the mean value between groups was tested with one-way analysis of variance (ANOVA); and $p < 0.05$ indicated that the difference between groups was statistically significant.

3. Results

3.1. Effects of SPJs on kidney morphology and function in aging rats

H&E staining showed that as compared with that in the 3-M group, in the 24-M group, some renal tubules of kidney were atrophic; compensatory dilatation appeared in the adjacent blood tubules; infiltration of inflammatory cells was observed in the surrounding mesenchyme; and protein casts showed up in some renal tubules. However, compared with the naturally aging group (24-M group), in both the SPJ-L and SPJ-H groups, the number of atrophied renal tubules, the number of inflammatory cells in the surrounding stroma and the protein casts in the renal tubules were reduced; and the morphological structures were improved (Fig. 1A). Masson's staining indicated that renal tubules, cytoplasm of interstitial cells and muscle fibers in the kidney were all stained in red, and the collagen fibers were blue. As compared with the 3-M group, renal collagen fibers of 24-M group were markedly increased. While compared with those of the 24-M group, renal collagen fibers of both SPJ-H and SPJ-L groups were significantly reduced (Fig. 1A and B). As compared with those in 3-M group, the levels of serum UA, Cys C and β 2-MG in 24-M group were

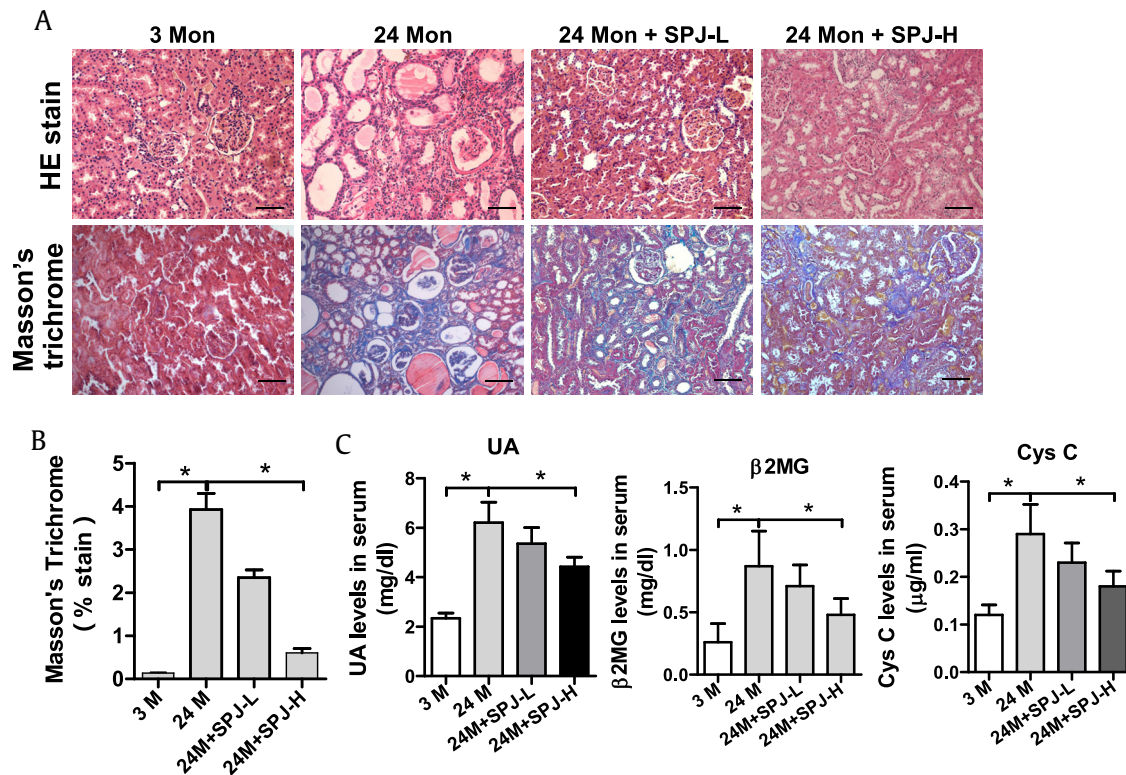


Fig. 1. Effects of SPJs on renal morphology and function in aging rats. (A) Representative images of H&E and Masson's trichrome stain of renal tissue (200 \times); (B) Average percentage of positive Masson's trichrome stained area (blue); and (C) The serum levels of UA, β 2MG, and Cys C were determined using ELISA. Data in (B) and (C) are expressed as mean \pm SD, * $p < 0.05$, $n = 6$.

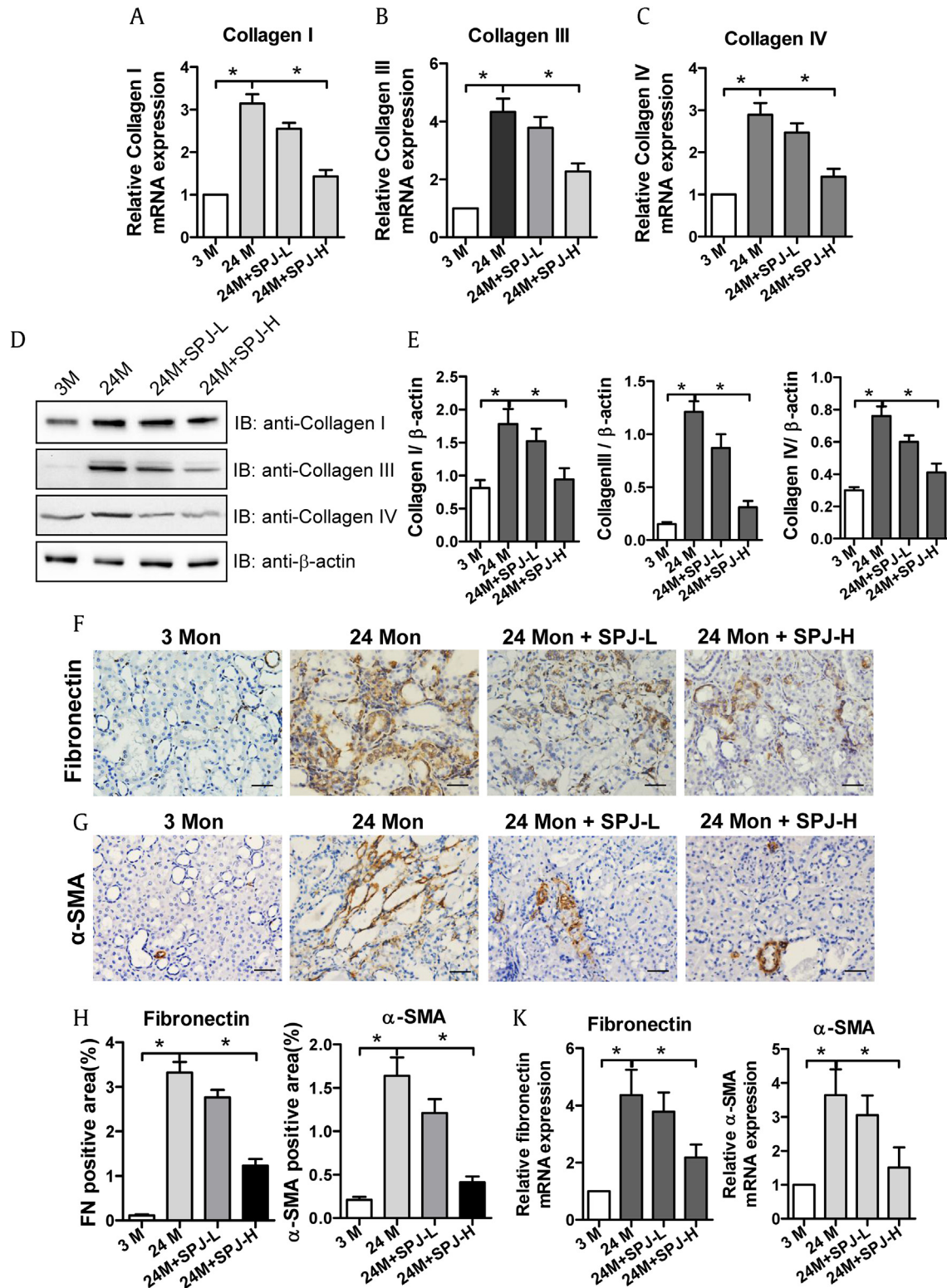


Fig. 2. Effects of SPJs on the expression levels of Collagen I, Collagen III, Collagen IV, Fibronectin and α -SMA in the renal tissue of aging rats. The mRNA expression level of Collagen I(A), Collagen III (B) and Collagen IV(C) were shown. (D), (E) Representative results of Western blot and quantitative analysis with antibodies against Collagen I, Collagen III and Collagen IV. β -actin was used as an internal control for normalization of protein loading. SPJs affected protein expression levels of Fibronectin (F) and α -SMA (G) in the renal tissue of aging rats as detected by immunohistochemistry (400 \times). (H) The quantitative analysis on protein expression levels (positive areas) of fibronectin and α -SMA in the kidneys. (K) The relative mRNA expression levels (folds) of Fibronectin and α -SMA in the kidneys. All the experiments were performed in triplicate. Data in (E), (H) and (K) are expressed as mean \pm SD, * p < 0.05, n = 6.

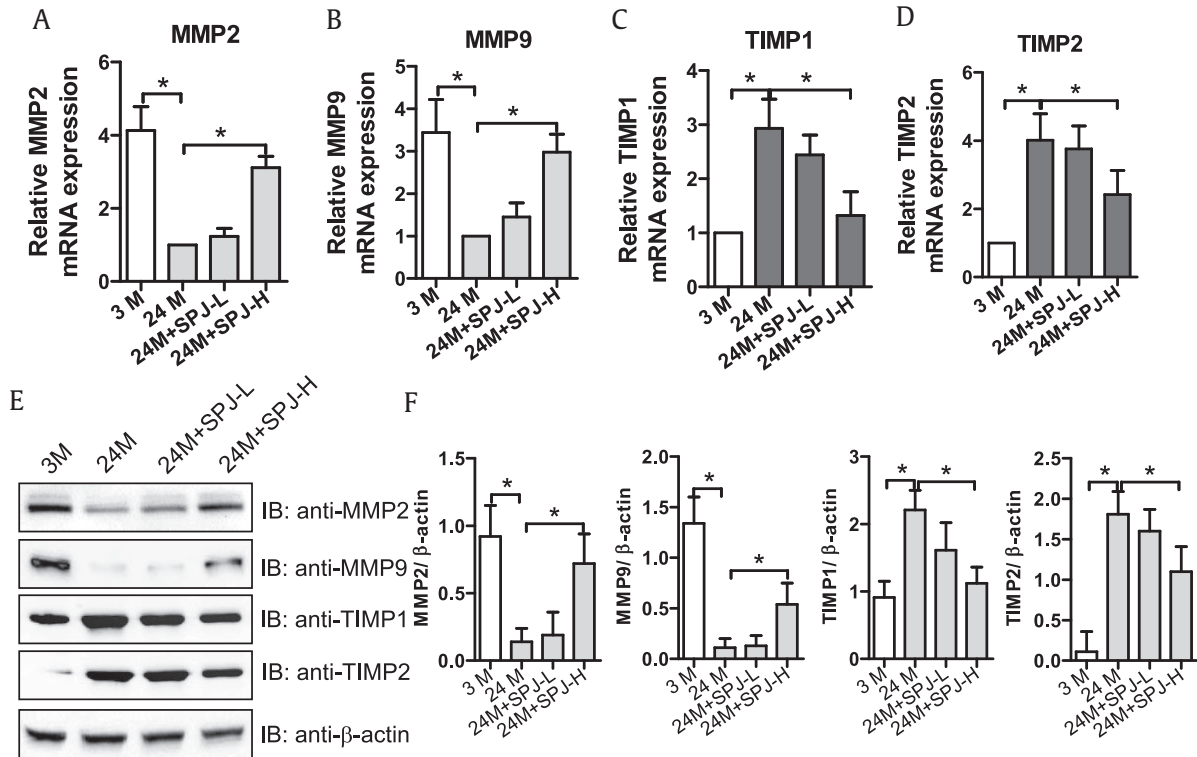


Fig. 3. Effects of SPJs on the expression levels of MMP2, MMP9, TIMP1 and TIMP2 in the renal tissue of aging rats. The mRNA expression levels of MMP2 (A), MMP9 (B), TIMP1 (C) and TIMP2 (D). (E) Effects of SPJs on the protein expression levels of MMP2, MMP9, TIMP1 and TIMP2 as detected with their specific antibodies via Western blot. Antibody against β -actin was used as an internal control for normalization of protein loading; (F) The quantitative relative protein expression levels of MMP2, MMP9, TIMP1 and TIMP2 based on Western blot. All the experiments were performed in triplicate. Data in (A-D) and (F) were expressed as mean \pm SD, * p < 0.05, n = 6.

observably increased (p < 0.05). Compared with those in the 24-M group, the levels of serum UA, Cys C and β 2-MG in the SPJ-H group were significantly decreased (p < 0.05) (Fig. 1C).

3.2. Effects of SPJs on expression levels of Collagen I, Collagen III and Collagen IV in renal tissues of aging rats

The results of Masson's staining described above showed that SPJs could significantly inhibit renal fibrosis associated with the natural senescence. Because deposition of ECM is the main feature of renal fibrosis, and Collagen I, Collagen III and Collagen IV are the major components of ECM, we next examined the effects of SPJs on the expression levels of collagen in renal tissues of aging rats. The mRNA expression levels of Collagen I (Fig. 2A), Collagen III (Fig. 2B), Collagen IV (Fig. 2C) and their corresponding protein levels (Fig. 2D and E) in the renal tissues of rats in the 24-M group were dramatically higher than those in the 3-M group (p < 0.05). As compared with those in the 24-M group, the expression levels of the corresponding genes at both mRNA and protein levels were all signally reduced (p < 0.05) in the renal tissues of rats in both SPJ-L and SPJ-H groups (Fig. 2).

3.3. Effects of SPJs on expression levels of fibronectin and α -SMA in kidney tissues of aged rats

Fibroblasts in the renal stroma are the primary producer of Collagen I, Collagen III and Collagen IV. Both fibronectin and α -SMA are the major hallmarks of fibroblast activation. Therefore, the effects of SPJs on the expression levels of Fibronectin and α -SMA in renal tissues of aging rats were examined. The results showed that protein expression levels (Fig. 2F-H) and mRNA expression levels

(Fig. 2K) of Fibronectin and α -SMA in the renal tissues of rats in 24-M group were significantly increased in comparison to 3-M group (p < 0.05). The protein expression levels (Fig. 2F-H) and mRNA expression levels (Fig. 2K) of both Fibronectin and α -SMA in the kidney tissues of rats in both SPJ-L and SPJ-H groups were significantly decreased with those in SPJ-H groups being more obvious as compared with 24-M group (p < 0.05).

3.4. Effects of SPJs on expression levels of MMP2, MMP9 and TIMP1 and TIMP2 in kidney tissues of aging rats

Degradation of ECM is catalyzed by MMPs, particularly MMP2 and MMP9, which are closely related to renal fibrosis. MMPs activities are basically inhibited by TIMPs, such as TIMP1 and TIMP2, which play a vital role in controlling ECM balance. As the results described above proved that SPJs could inhibit ECM deposition. Next, we tested the effects of SPJs on the expression of MMP2, MMP9, TIMP1 and TIMP2 in renal tissues of aging rats. As shown in Fig. 3, the levels of mRNA and proteins of MMP2 and MMP9 were memorably lessened in the renal tissues of 24-M group as compared with those in 3-M group, while those of TIMP1 and TIMP2 were markedly aggrandized (Fig. 3) (p < 0.05). However, in renal tissues of rats in both SPJ-L and SPJ-H groups, the mRNA and protein expression levels of MMP2 and MMP9 were dose-dependently and significantly increased in comparison to those in 24-M group, while the mRNA and protein expression levels of TIMP1 and TIMP2 were dose-dependently and significantly decreased (Fig. 3) (p < 0.05).

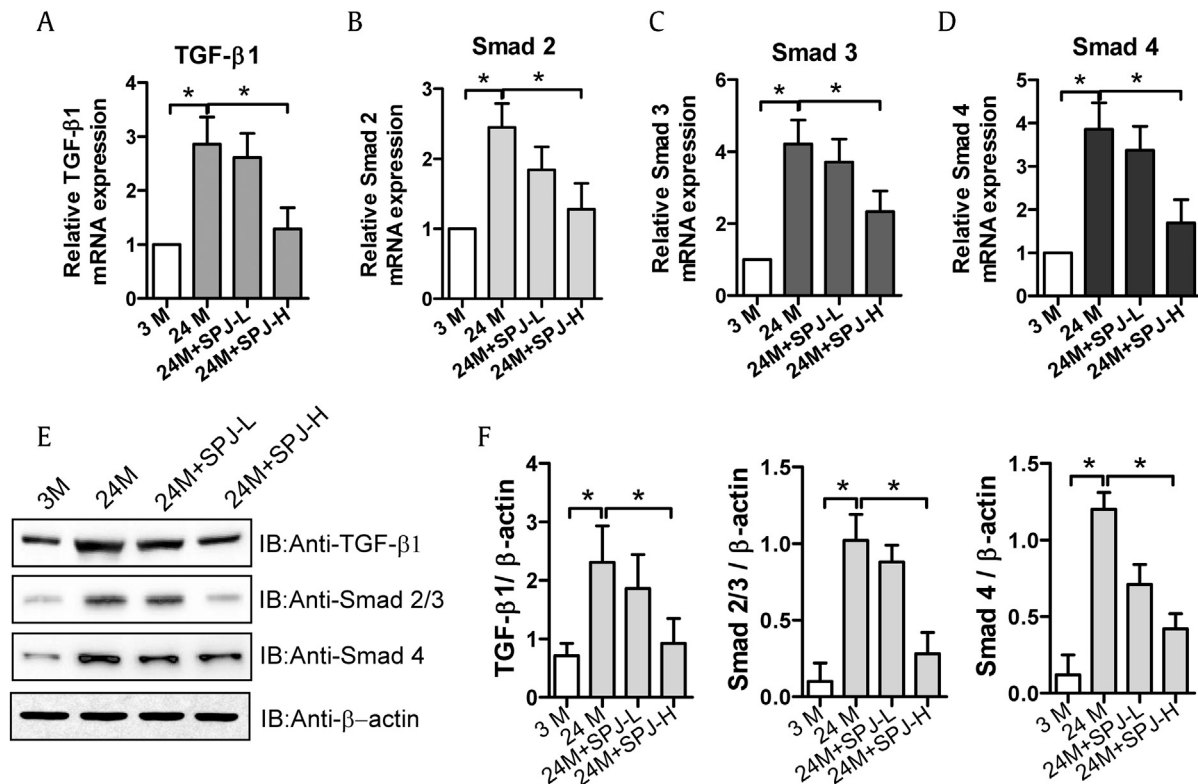


Fig. 4. Effects of SPJs on expression levels of genes involved in TGF-β1/Smad signaling in the renal tissue of aging rats. The mRNA expression levels of TGF-β1 (A), Smad2(B), Smad3(C), and Smad4(D). (E) Representative results of Western blot analysis with antibodies against TGF-β1, Smad2/3, and Smad4, β-actin was used as a control; and (F) The quantitative relative protein expression levels of MMP2, MMP9, TIMP1 and TIMP2 based on Western blot. All the experiments were performed in triplicate. Data in (A-D) and (F) were expressed as mean \pm SD, * $p < 0.05$, $n = 6$.

3.5. Effects of SPJs on TGF-β1/Smad signaling pathway in renal tissues of aging rats

In renal fibrosis, TGF-β1 can induce phosphorylation of members of Smad family, among which Smad-2, Smad-3 and Smad-4 play a vital role in TGF-β1/Smad signaling. Next, we examined the effects of SPJs on the proteins involved in TGF-β1/Smad signaling pathway in renal tissues of aging rats. As shown in Fig. 4, as compared with those in 3-M group, the mRNA (Fig. 4A–D) and protein (Fig. 4E and F) expression levels of TGF-β1, Smad2, Smad3, and Smad4 in the kidney tissues of 24-M group were prominently increased ($p < 0.05$). However, the mRNA (Fig. 4A–D) and protein (Fig. 4E and F) levels of TGF-β1, Smad2, Smad3, and Smad4 in renal tissues of rats in both SPJ-L and SPJ-H groups were memorably decreased when compared with those in 24-M group ($p < 0.05$) with those in SPJ-H group being decreased more obviously.

3.6. Effects of SPJs on expression levels of inflammatory factors and NF-κB signaling pathway in renal tissues of aging rats

The process of aging is frequently accompanied by the occurrence of renal inflammation, which is intimately bound up with renal fibrosis. NF-κB-induced inflammatory cytokines are of important meaning in mediating the inflammatory response. In order to determine whether the reduction of renal fibrosis caused by SPJs in aging process is causally related to their effects on inhibition of renal inflammation, we explored the effects of SPJs on expression levels of inflammatory cytokines. As shown in Fig. 5, both mRNA and protein expression levels of IL-1β, TNF-α, and IL-6 in the renal tissues of 24-M group were remarkably enhanced while

compared with 3-M group ($p < 0.05$) (Fig. 5A and B); As compared with those in natural aging group (24-M group), both mRNA and protein expression levels of IL-1β, IL-6 and TNF-α in the renal tissues of rats in SPJ-H group were notably reduced ($p < 0.05$) (Fig. 5A and B). As compared with those in 3-M group, the levels of phosphorylated NF-κB and IκB proteins in the renal tissues of 24-M group were observably and significantly elevated ($p < 0.05$) (Fig. 5C); and the levels of phosphorylated NF-κB and IκB proteins in both SPJ-L and SPJ-H groups were significantly decreased in comparison to those in 24-M group ($p < 0.05$) (Fig. 5C) with those in SPJ-H groups being decreased more notably.

3.7. Effects of SPJs on responding to oxidative stress and Nrf2-ARE signaling in renal tissues of aging rats

Oxidative stress is involved in age-related renal fibrosis, and the Nrf2-ARE signaling can participate in regulating cellular oxidative stress. Among them, ROS (i.e. MDA and LPO) and both enzymatic and non-enzymatic antioxidants (such as GSH, GSH-PX, CAT, and SOD) play different roles in responding to oxidative stress. Thus, we next explored the effects of SPJs on the levels of ROS, antioxidants and Nrf2-ARE signaling in renal tissues of aging rats. As shown in Fig. 6A, as compared with those in 3-M group, the levels of MDA and LPO in renal tissues of rats in 24-M group were dramatically increased ($p < 0.05$), while those of MDA and LPO in renal tissues of rats in SPJ-L and SPJ-H group were significantly reduced in comparison to those in 24-M group ($p < 0.05$). The levels of antioxidant enzymes, including CAT, SOD, and antioxidants, including GSH and GSH-PX, in the renal tissues of rats in 24-M group were memorably reduced when compared with 3-M group ($p < 0.05$), and in the

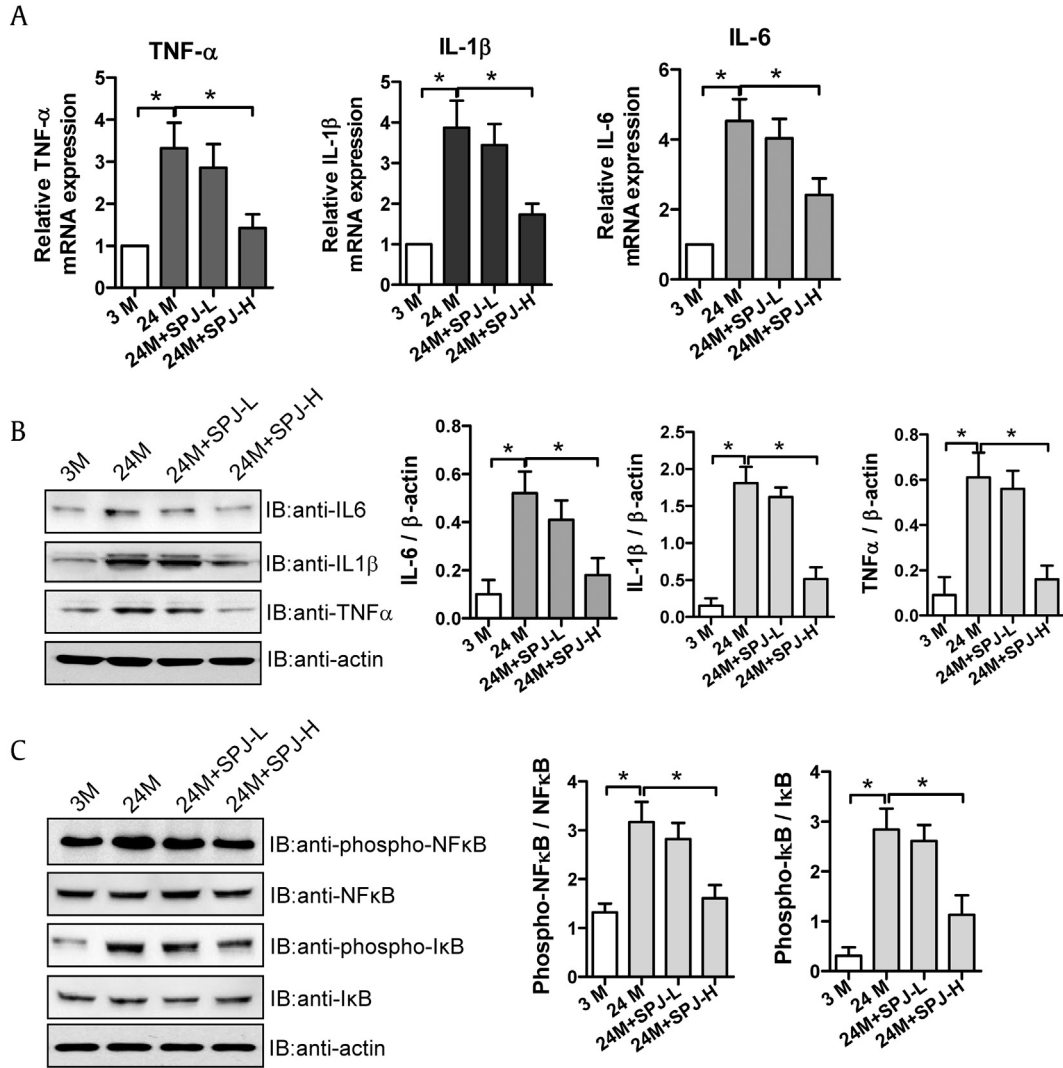


Fig. 5. Effects of SPJs on the expression levels of inflammatory factors and NF- κ B signaling in the renal tissue of aging rats. (A) The mRNA expression levels of TNF- α , IL-1 β and IL-6 detected by real time PCR. (B) Representative results of Western blot and quantitative analysis with antibodies against TNF- α , IL-1 β and IL-6; β -actin was used as an internal control for normalization of protein loading; (C) Representative results of Western blot and quantitative analysis with antibodies against NF- κ B, I κ B, and the phosphorated NF- κ B, I κ B, β -actin was used as the internal control for normalization of loading control. All the experiments were performed in triplicate. Data in (A-C) were expressed as mean \pm SD, * p < 0.05, n = 6.

renal tissues of rats in SPJ-H group were dramatically increased in comparison to 24-M group (p < 0.05) (Fig. 6A). Through compared with 3-M group, both mRNA and protein expression levels of Nrf2, HO-1 and NQO1 in the renal tissues of 24-M group were prominently decreased (p < 0.05); As compared with the natural aging group, the mRNA and protein expression levels of Nrf2, HO-1 and NQO1 in the kidney tissues of rats in both SPH-L and SPJ-H groups were notably enhanced (p < 0.05) with those in SJP-H group being decreased more dramatically.

4. Discussion

Renal interstitial fibrosis is an inhibitory pathological manifestation of many chronic kidney diseases developing to terminal stage, and is also one of the main manifestations of aging kidneys and one of the main causes of renal failure. In the etiology of renal aging, some renal structural changes, such as the increased renal interstitial fibrosis, take place with aging [23]. The results obtained from present study indicated that treatment of aging rats with SPJs,

especially at high dose, could significantly improve the declined renal function and renal interstitial fibrosis in aging rats (Fig. 1). Furthermore, we also gained significant insights into the mechanisms underlying the protective effects of SPJs on improvement of renal functions and renal interstitial fibrosis.

ECM accumulation has been acknowledged to be the eventual pathway of renal fibrosis caused by aging [24]. To evaluate the effect of SPJs treatment on ECM accumulation, we analyze the collagen deposition in the kidney with Masson's trichrome staining and the result indicated that the renal interstitial collagen deposition in the kidney of aging rats was significantly reduced after being treated with high-dose of SPJs (Fig. 1A and B). Collagen I, Collagen III and Collagen IV are major components of ECM and they are deposited in the kidney during interstitial fibrosis. Their mRNA expression levels were examined with real time PCR and protein expression levels were monitored by western blot with corresponding antibodies. The results showed that the increased expressions of mRNA and protein of Collagen I, Collagen III and Collagen IV caused by aging were all significantly reduced after being treated with high-dose of

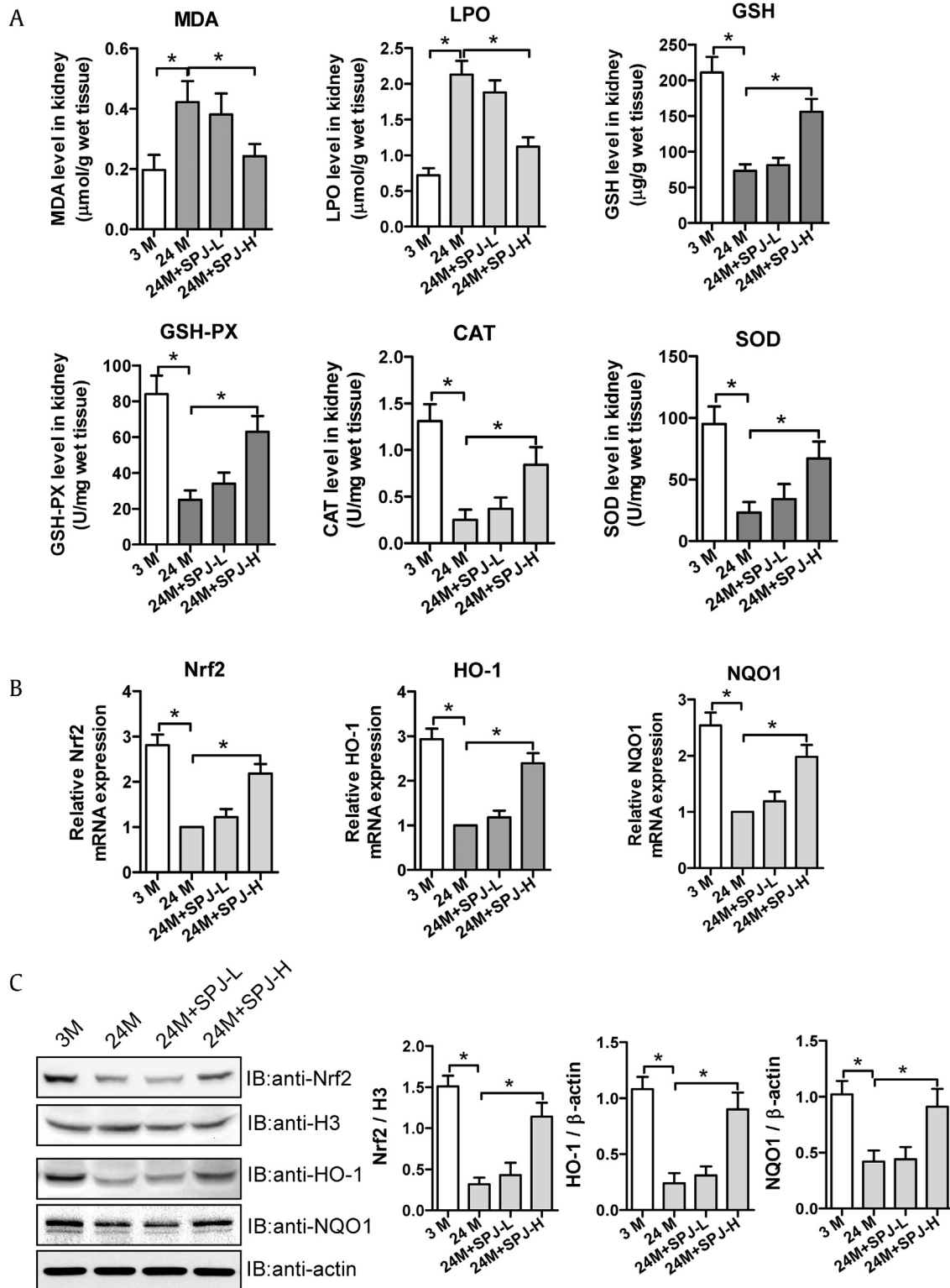


Fig. 6. Effects of SPJs on oxidative stress parameters and Nrf2-ARE signaling in the renal tissue of aging rats. (A) Relative levels of oxidative stress parameters MDA, LPO, GSH, GSH-PX, CAT and SOD measured with corresponding kits. (B) The relative mRNA expression levels of Nrf2, HO-1 and NQO1 detected by real time PCR. (C) Representative results of Western blot and quantitative analysis with antibodies against Nrf2, HO-1 and NQO1, β -actin and H3 were used as internal control for normalization of the loading control, respectively. All the experiments were performed in triplicate. Data in (A-C) were expressed as mean \pm SD, * p < 0.05, n = 6.

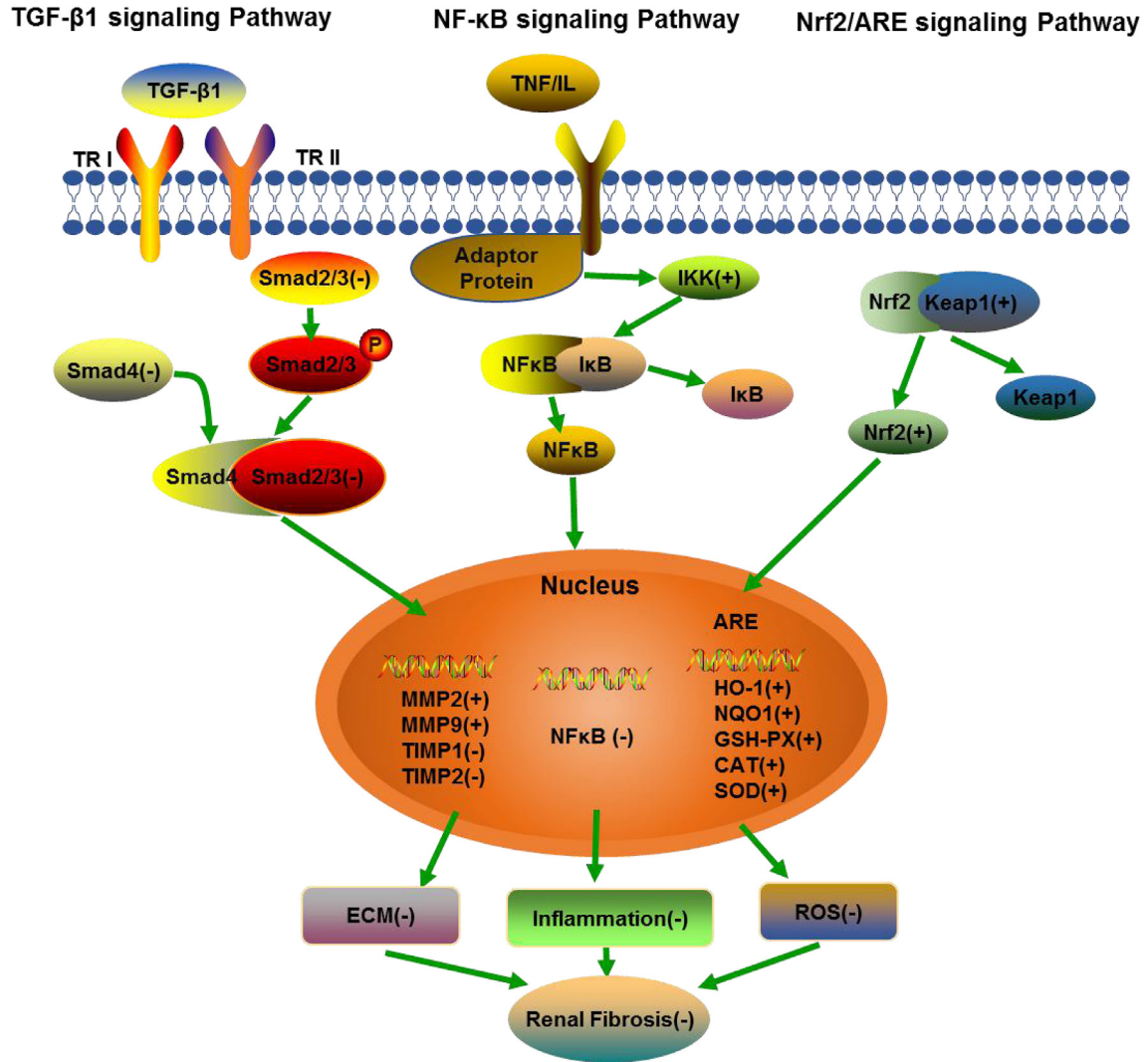


Fig. 7. Schematic illustration for summary of the regulatory effects of SPJs on TGF-β1/Smad signaling, NF-κB signaling and Nrf2-ARE signaling pathway. (+): positive effect, (-): negative effect.

SPJs, indicating that SPJs are capable of reducing ECM accumulation in renal tissues and thus, alleviating renal fibrosis associated with aging.

Fibroblasts in renal stroma are regarded as the major producer of fibrous matrix, for instance Collagen I, Collagen III and Collagen IV. Fibronectin (FN) and α-SMA are two hallmarks of activation of fibroblasts [25]. Then, by applying immunohistochemistry method, we detected the levels of FN and α-SMA in the kidney of aging rats. As shown in Fig. 2F–K, the increased levels of FN and α-SMA caused by aging were significantly reduced in renal tissues of rats after being treated with high-dose of SPJs, indicating that SPJs are capable of activating fibroblasts in the renal stroma.

It was previously revealed that degradation of ECMs is mediated chiefly by matrix metalloproteinases (MMPs), including collagenases, matrilysins, etc. [26,27], especially MMP2 and MMP9, which are correlated to renal fibrosis [28]. Nevertheless, the activities of MMPs are reduced by TIMPs. In the TIMPs family, both TIMP1 and TIMP2 can inhibit the activities of MMPs, thus playing a pivotal role in controlling the balance between ECM accumulation and degradation [29]. For instance, Sharma et al reported that the degradation of Collagen IV was inhibited when TIMPs were up-regulated while MMPs were down-regulated in renal fibrosis, thereby

promoting ECM accumulation [30]. The results obtained from this study showed that in the kidney of aging rats, both mRNA and protein expression levels were reduced in MMP2 and MMP9 and were increased in TIMP1 and TIMP2. After being treated with high-dose of SPJs, the mRNA and protein expression levels of MMP2 and MMP9 were increased in, while those of TIMP1 and TIMP2 were reduced (Fig. 3). These results reveal that in renal fibrosis induced by senescence and ECM accumulation are usually accompanied with changes in the expression levels of MMPs and TIMPs. Thus, SPJs can control the balance between TIMPs and MMPs.

An increasing evidence has suggested that abnormal activation of TGF-β1/Smad signaling pathway is a major cause leading to renal fibrosis [31]. After binding to TGF-β type II receptor (TβRII), TGF-β1 works via signal cascades. TβRII can phosphorylates TGF-β type I receptor (TβFI). Subsequently, both TβFI and TβRII form heterotetrameric complexes, leading to Smad2/3 phosphorylation. The phosphorylated Smad2/3 then binds to Smad4 to form Smad complexes, which can transfer into the nucleus within which they are involved in regulating the transcription of their target gene [32]. Our results showed that while aging rats were treated with SPJs at high-dose, they could significantly reduce both mRNA and protein expression levels of TGF-β1, Smad2/3 and Smad4 associated with

aging, indicating that SPJs are capable of negatively regulating TGF- β 1/Smad signaling (Fig. 4).

Aging can induce inflammation response, which plays a key part in the development of renal fibrosis. It has been pointed out that during aging, inflammatory mediators, such as TNF- α , are released, which, in turn, can activate fibroblasts to initiate renal fibrosis [33,34]. Therefore, we determined whether SPJs could inhibit inflammatory response induced by senescence and subsequent renal fibrosis. Our data clearly showed that SPJs at the high-dose could significantly inhibit the mRNA and protein expression levels of a number of inflammatory mediators, for instance IL-1 β , IL-6 and TNF- α , in renal tissues of aging rats (Fig. 5A and B), demonstrating that SPJs can directly suppress the inflammatory response. Thus, treatment with SPJs can improve renal interstitial fibrosis in aging rats, at least in part, by inhibiting the inflammatory response. NF- κ B signaling pathway plays a vital role in inflammatory response [35,36]. Our results showed that SPJs treatment can effectively inhibit the phosphorylation of I κ B in renal tissues of aging rats, and then inhibit the activation of NF- κ B signaling pathway (Fig. 5C). These results provide further support for the roles of SPJs in suppression of inflammation response and renal fibrosis via inhibiting NF- κ B signal pathway.

Oxidative stress associated with renal fibrosis includes the increased level of ROS and the reduced antioxidant capacity [37]. Oxidative stress is one of the mechanisms involved in senescence related renal fibrosis. An increasing lines of evidence have suggested that oxidative stress is engaged in the increased lipid peroxidation [38], which leads to increased generation of MDA and LPO. On the other hand, Nrf2 has been known to be a critical transcription factor responsible for mediating anti-oxidant responses against oxidative stress by regulating its downstream antioxidant enzymes [39]. Activation of Nrf2-ARE signaling pathway has been reported to improve fibrosis of organ [40,41]. Like NF- κ B, Nrf2 is normally localized in the cytoplasm where it is coupled with Keap1; under oxidative stress, Keap1 activity is weakened, and then Nrf2 can escape from the degradation mediated by Keap1, so as to shift and activate the transcription corresponding target antioxidant genes in the nucleus [42]. It has been reported that PPAR α agonist, fenofibrate, improves age-related renal injury through AMPK/SIRT1 signal pathway that activation of AMPK and SIRT1 results in simultaneous deacetylation and phosphorylation of their target molecules, and decreases the kidney's sensitivity to age-related changes. In the present study, we demonstrated that Saponins from *Panax japonicus* (SPJs) were capable of regulating the levels of the activities of several antioxidant enzymes, including CAT, SOD, GSH-px, and non-enzymatic antioxidants (e.g. GSH), which are related to alleviation of oxidative stress, and to improvement of age-related renal fibrosis by Nrf2-ARE pathway [43].

Chronic inflammation and oxidative stress are the main mechanisms of age-related renal fibrosis. Qiao et al reported that dioscin, a natural steroid saponin isolated from herbal plants, possessed a protective effect against fructose-caused kidney damage, including fibrosis and inflammation, etc. [44]. Similarly, we found that SPJs regulated inflammatory cytokines, including TNF- α , IL-1 β , and IL-6 through TGF- β 1/Smad signaling pathway to improve renal fibrosis. Dioscin is also able to regulate the levels of MDA, SOD and GSH-PX, and reduce the ROS level by Sirt3 signaling pathway in renal tissue. In this study, we found that SPJs improved inflammation by TGF- β 1/Smad signaling pathway and oxidative stress by Nrf2-ARE signaling pathway. Furthermore, in our current research, we observed that SPJs treatment could significantly reduce the levels of and LPO and MDA in renal tissues of aging rats, increase the activities and expression levels of antioxidant enzymes, including CAT and SOD, and enhancing the levels of non-enzymatic antioxidants,

including GSH, and GSH-PX, and also increase the expression levels of Nrf2, HO-1 and NQO1 (Fig. 6). These results indicate that the protective effects of SPJs on renal fibrosis may be, at least in part, resulted from its activation of Nrf2-ARE signaling, thereby reducing ROS stress.

In conclusion, our study has clearly demonstrated that SPJs can reduce renal fibrosis associated with aging via simultaneously inhibiting the TGF- β 1/Smad, NF- κ B signaling pathway and activating the Nrf2-ARE signaling pathway (Fig. 7) and that SPJs can be used as a potentially valuable anti-renal fibrosis drug.

Conflicts of interest

The authors declare that there are no conflict of interest.

Acknowledgments

This study was financially supported by grants from National Natural Science Foundation of China (Grant No. 81773959 to C.F. Yuan and No. 81974528 to C.F. Yuan) and Health Commission of Hubei Province Scientific Research Project in China. (Grant No. WJ2019H527 to C.F. Yuan)

Appendix A. Supplementary data

Supplementary data to this article can be found online at <https://doi.org/10.1016/j.jgr.2020.08.005>.

References

- Rule AD, Amer H, Cornell LD, Taler SJ, Cosio FG, Kremers WK, Textor SC, Stegall MD. The association between age and nephrosclerosis on renal biopsy among healthy adults. *Ann Intern Med* 2010;152(9):561–7.
- Xie L, Cianciolo RE, Hulette B, Lee HW, Qi Y, Cofer G, Johnson GA. Magnetic resonance histology of age-related nephropathy in the Sprague Dawley rat. *Toxicol Pathol* 2012;40(5):764–78.
- Luyckx VA, Tonelli M, Stanifer JW. The global burden of kidney disease and the sustainable development goals. *Bull World Health Organ* 2018;96(6):414–422D.
- Portilla D. Apoptosis, fibrosis and senescence. *Nephron Clin Pract* 2014;127(1–4):65–9.
- Zhou X, Zhang J, Xu C, Wang W. Curcumin ameliorates renal fibrosis by inhibiting local fibroblast proliferation and extracellular matrix deposition. *J Pharmacol Sci* 2014;126(4):344–50.
- Ni WJ, Ding HH, Zhou H, Qiu YY, Tang LQ. Renoprotective effects of berberine through regulation of the MMPs/TIMPs system in streptozocin-induced diabetic nephropathy in rats. *Eur J Pharmacol* 2015;764:448–56.
- Lan HY. Diverse roles of TGF-beta/Smads in renal fibrosis and inflammation. *Int J Biol Sci* 2011;7(7):1056–67.
- Lan HY, Chung AC. TGF-beta/Smad signaling in kidney disease. *Semin Nephrol* 2012;32(3):236–43.
- Montecino-Rodriguez E, Berent-Maoz B, Dorshkind K. Causes, consequences, and reversal of immune system aging. *J Clin Invest* 2013;123(3):958–65.
- Shaw AC, Goldstein DR, Montgomery RR. Age-dependent dysregulation of innate immunity. *Nat Rev Immunol* 2013;13(12):875–87.
- Adler AS, Kawahara TL, Segal E, Chang HY. Reversal of aging by NFkappaB blockade. *Cell Cycle* 2008;7(5):556–9.
- Perkins ND. Integrating cell-signalling pathways with NF-kappaB and IKK function. *Nat Rev Mol Cell Biol* 2007;8(1):49–62.
- Hoffmann A, Natoli G, Ghosh G. Transcriptional regulation via the NF-kappaB signaling module. *Oncogene* 2006;25(51):6706–16.
- Siems W, Quast S, Carluccio F, Wiswedel I, Hirsch D, Augustin W, Hampi H, Riehle M, Sommerburg O. Oxidative stress in chronic renal failure as a cardiovascular risk factor. *Clin Nephrol* 2002;58(Suppl 1):S12–9.
- Al-Sheikh YA, Ghneim HK, Aljaser FS, Aboul-Soud MAM. Ascorbate ameliorates *Echis coloratus* venom-induced oxidative stress in human fibroblasts. *Exp Ther Med* 2017;14(1):703–13.
- Yuan C, Wang C, Bu Y, Xiang T, Huang X, Wang Z, Yi F, Ren G, Liu G, Song F. Antioxidative and immunoprotective effects of *Pyracantha fortuneana* (Maxim.) Li polysaccharides in mice. *Immunol Lett* 2010;133(1):14–8.
- Hyun SH, Kim SW, Seo HW, Youn SH, Kyung JS, Lee YY, In G, Park CK, Han CK. Physiological and pharmacological features of the non-saponin components in Korean Red Ginseng. *J Ginseng Res* 2020;44(4):527–37.
- Song YN, Yuan D, Zhang CC, Wang LP, He YM, Wang T, Zhou ZY. Effect of saponins extracted from *Panax japonicus* on inhibiting cardiomyocyte

- apoptosis by AMPK/Sirt1/NF- κ B signaling pathway in aging rats. *Zhongguo Zhong Yao Za Zhi* 2017;42(23):4656–60.
- [19] Deng LL, Yuan D, Zhou ZY, Wan JZ, Zhang CC, Liu CQ, Dun YY, Zhao HX, Zhao B, Yang YJ, et al. Saponins from *Panax japonicus* attenuate age-related neuroinflammation via regulation of the mitogen-activated protein kinase and nuclear factor kappa B signaling pathways. *Neural Regen Res* 2017;12(11):1877–84.
- [20] Wang T, Di G, Yang L, Dun Y, Sun Z, Wan J, Peng B, Liu C, Xiong G, Zhang C, et al. Saponins from *Panax japonicus* attenuate D-galactose-induced cognitive impairment through its anti-oxidative and anti-apoptotic effects in rats. *J Pharm Pharmacol* 2015;67(9):1284–96.
- [21] Wei N, Zhang C, He H, Wang T, Liu Z, Liu G, Sun Z, Zhou Z, Bai C, Yuan D. Protective effect of saponins extract from *Panax japonicus* on myocardial infarction: involvement of NF- κ B, Sirt1 and mitogen-activated protein kinase signalling pathways and inhibition of inflammation. *J Pharm Pharmacol* 2014;66(11):1641–51.
- [22] He H, Xu J, Xu Y, Zhang C, Wang H, He Y, Wang T, Yuan D. Cardioprotective effects of saponins from *Panax japonicus* on acute myocardial ischemia against oxidative stress-triggered damage and cardiac cell death in rats. *J Ethnopharmacol* 2012;140(1):73–82.
- [23] Karam Z, Tuazon J. Anatomic and physiologic changes of the aging kidney. *Clin Geriatr Med* 2013;29(3):555–64.
- [24] Tang R, Zhou QL, Ao X, Peng WS, Veeraragoo P, Tang TF. Fosinopril and losartan regulate klotho gene and nicotinamide adenine dinucleotide phosphate oxidase expression in kidneys of spontaneously hypertensive rats. *Kidney Blood Press Res* 2011;34(5):350–7.
- [25] Pang M, Kothapally J, Mao H, Tolbert E, Ponnusamy M, Chin YE, Zhuang S. Inhibition of histone deacetylase activity attenuates renal fibroblast activation and interstitial fibrosis in obstructive nephropathy. *Am J Physiol Renal Physiol* 2009;297(4):F996–f1005.
- [26] Back M, Ketelhuth DF, Agewall S. Matrix metalloproteinases in atherothrombosis. *Prog Cardiovasc Dis* 2010;52(5):410–28.
- [27] Thrailkill KM, Clay Bunn R, Fowlkes JL. Matrix metalloproteinases: their potential role in the pathogenesis of diabetic nephropathy. *Endocrine* 2009;35(1):1–10.
- [28] Racca MA, Novoa PA, Rodriguez I, Della Vedova AB, Pellizas CG, Demarchi M, Donadio AC. Renal dysfunction and intragraft proMMP9 activity in renal transplant recipients with interstitial fibrosis and tubular atrophy. *Transpl Int* 2015;28(1):71–8.
- [29] Visse R, Nagase H. Matrix metalloproteinases and tissue inhibitors of metalloproteinases: structure, function, and biochemistry. *Circ Res* 2003;92(8):827–39.
- [30] Sharma AK, Mauer SM, Kim Y, Michael AF. Altered expression of matrix metalloproteinase-2, TIMP-1, and TIMP-2 in obstructive nephropathy. *J Lab Clin Med* 1995;125(6):754–61.
- [31] Yao Z, Yang S, He W, Li L, Xu R, Zhang X, Li H, Zhan R, Sun W, Tan J, et al. P311 promotes renal fibrosis via TGFbeta1/Smad signaling. *Sci Rep* 2015;5:17032.
- [32] Choi ME, Ding Y, Kim SI. TGF-beta signaling via TAK1 pathway: role in kidney fibrosis. *Semin Nephrol* 2012;32(3):244–52.
- [33] Wada T, Sakai N, Matsushima K, Kaneko S. Fibrocytes: a new insight into kidney fibrosis. *Kidney Int* 2007;72(3):269–73.
- [34] Misseri R, Meldrum DR, Dagher P, Hile K, Rink RC, Meldrum KK. Unilateral ureteral obstruction induces renal tubular cell production of tumor necrosis factor-alpha independent of inflammatory cell infiltration. *J Urol* 2004;172(4 Pt 2):1595–9. discussion 1599.
- [35] Chaves de Souza JA, Nogueira AV, Chaves de Souza PP, Kim YJ, Silva Lobo C, Pimentel Lopes de Oliveira GJ, Cirelli JA, Garlet GP, Rossa Jr C. SOCS3 expression correlates with severity of inflammation, expression of proinflammatory cytokines, and activation of STAT3 and p38 MAPK in LPS-induced inflammation in vivo. *Mediators Inflamm* 2013;2013:650812.
- [36] Kyriakis JM, Avruch J. Mammalian MAPK signal transduction pathways activated by stress and inflammation: a 10-year update. *Physiol Rev* 2012;92(2):689–737.
- [37] Qin T, Yin S, Yang J, Zhang Q, Liu Y, Huang F, Cao W. Sinomenine attenuates renal fibrosis through Nrf2-mediated inhibition of oxidative stress and TGF β signaling. *Toxicol Appl Pharmacol* 2016;304:1–8.
- [38] Abdelkhalek NK, Ghazy EW, Abdel-Daim MM. Pharmacodynamic interaction of *Spirulina platensis* and deltamethrin in freshwater fish Nile tilapia, *Oreochromis niloticus*: impact on lipid peroxidation and oxidative stress. *Environ Sci Pollut Res Int* 2015;22(4):3023–31.
- [39] Wasik U, Milkiewicz M, Kempinska-Podhorodecka A, Milkiewicz P. Protection against oxidative stress mediated by the Nrf2/Keap1 axis is impaired in Primary Biliary Cholangitis. *Sci Rep* 2017;7:44769.
- [40] Chen Z, Xie X, Huang J, Gong W, Zhu X, Chen Q, Huang J, Huang H. Connexin43 regulates high glucose-induced expression of fibronectin, ICAM-1 and TGF-beta1 via Nrf2/ARE pathway in glomerular mesangial cells. *Free Radic Biol Med* 2017;102:77–86.
- [41] Zhou W, Mo X, Cui W, Zhang Z, Li D, Li L, Xu L, Yao H, Gao J. Nrf2 inhibits epithelial-mesenchymal transition by suppressing snail expression during pulmonary fibrosis. *Sci Rep* 2016;6:38646.
- [42] Lacher SE, Slattery M. Gene regulatory effects of disease-associated variation in the NRF2 network. *Curr Opin Toxicol* 2016;1:71–9.
- [43] Kim EN, Lim JH, Kim MY, Kim HW, Park CW, Chang YS, Choi BS. PPARalpha agonist, fenofibrate, ameliorates age-related renal injury. *Exp Gerontol* 2016;81:42–50.
- [44] Qiao Y, Xu L, Tao X, Yin L, Qi Y, Xu Y, Han X, Tang Z, Ma X, Liu K, et al. Protective effects of dioscin against fructose-induced renal damage via adjusting Sirt3-mediated oxidative stress, fibrosis, lipid metabolism and inflammation. *Toxicol Lett* 2018;284:37–45.